Proton Interactions with Hemes *a* and a_3 in Bovine Heart Cytochrome *c* Oxidase[†]

Dzmitry Parul, Graham Palmer, and Marian Fabian*

Department of Biochemistry and Cell Biology, MS 140, Rice University, 6100 Main Street, Houston, Texas 77005

Received July 22, 2004; Revised Manuscript Received December 9, 2004

ABSTRACT: Three forms of cytochrome *c* oxidase, fully oxidized CcO (CcO−O), oxidized CcO complexed with cyanide (CcO·CN), and mixed valence CcO, in which both heme a_3 and Cu_B are reduced and stabilized by carbon monoxide (MV·CO), were investigated by optical spectroscopy, MCD, and stopped-flow for the pH sensitivity of spectral features. In the pH range between pH 5.7 and 9.0, both heme *a* and heme a_3 in CcO−O interact with a single protolytic group. From the variation of the position of the Soret peak with changes in pH, a pK_a of 6.6 ± 0.2 was determined for this group. The pH sensitivity of heme a_3 is lost in the CcO·CN complex, and only heme *a* responds to pH changes. In MV·CO the spectra of both hemes are almost independent of pH between 5.7 and 11.0. The stoichiometry of proton uptake in the conversion of CcO−O both to MV·CO and to fully reduced CcO was determined between pH 5.8 and pH 8.2. Formation of MV·CO from CcO−O was accompanied by the uptake of approximately two protons, and this value was almost independent of pH. Full reduction of oxidized CcO was associated with the uptake of approximately 2 H^+ at basic pH, and this value increases with decreasing pH. On the basis of these proton uptake measurements, it is concluded that the pK_a of the group is independent of the redox state of CcO. It is suggested that Glu60 of subunit II, located at the entrance of the proton conducting K-channel, is the protolytic residue that interacts with both hemes through a hydrogen-bonding network.

The respiratory heme-copper oxidases constitute a superfamily of terminal oxidases in both prokaryotic organisms and the mitochondria of eukaryotic cells. Mitochondrial cytochrome *c* oxidase (CcO)[1] is an integral membrane protein that catalyzes the reduction of molecular oxygen to water using the reducing equivalents supplied by ferrocytochrome *c*. Four redox centers of CcO are involved in electron transfer from cytochrome *c* to dioxygen. Cu_A and heme *a* are primary electron acceptors, and electrons from these sites are delivered to the binuclear center of CcO, consisting of heme a_3 and Cu_B, where oxygen is reduced to water.

This chemical reaction is associated with the generation of a transmembrane proton gradient by two different processes. The first is the oxidation of cytochrome *c* from the cytosolic side coupled to the proton consumption from the matrix side that is required for water formation. The second process involves the translocation of protons from the matrix to the cytosolic side and is referred to as proton pumping.

Mitochondrial CcO consists of 13 subunits (*1*), but the redox centers are localized in subunits I and II. The X-ray structure reveals that heme *a*, heme a_3, and Cu_B are positioned in subunit I, Cu_A is in subunit II, and all four redox centers are buried within the protein (*2*). In the structure of fully oxidized bovine CcO (CcO−O) the possible proton conducting channels connecting the redox centers with the bulk aqueous phase are interrupted (*2*). Despite the isolation of the redox centers from the solution by protein the optical spectrum of oxidized CcO is sensitive to variations in pH (*3*, *4*). It was previously observed that, following a change in pH, the spectrum of CcO−O responds in two kinetically distinct phases (*4*) and heme a_3 was identified as the pH-sensitive chromophore (*3*, *4*). From the changes in the apparent equilibrium position of the Soret band, required up to several hours for completion, the interaction between heme a_3 and a single protolytic group with a pK_a of 7.8 was deduced (*4*). The presence of two phases of spectral changes was interpreted as reflecting two populations of CcO−O with different proton accessibility to heme a_3 (*4*).

Another group with a pK_a of 6.5−6.9 was identified in the reaction of both cyanide and hydrogen peroxide with oxidized heme a_3 (*5*−*8*). It was concluded that only the form of CcO that has this group protonated can react with cyanide and that the reaction is dependent on the pH inside the mitochondria (*7*).

In the reaction of oxidized CcO with hydrogen peroxide two catalytic intermediates, called "peroxy" (P) and ferryl (F), are produced. The pH-dependent yield of P implicated a group with a pK_a of 6.8 (*8*). A very similar pK_a for a group that regulates the yield of both P and F forms was also observed in our recent study (*9*).

[†] Supported by the National Institutes of Health (GM 55807) and the Robert A. Welch Foundation (C-636).

* To whom correspondence should be addressed. E-mail: fabian@rice.edu; voice: 713-348-2373; fax: 713-348-5365.

[1] Abbreviations: cytochrome *c* oxidase (CcO); oxidized CcO (CcO−O); complex of oxidized CcO with cyanide (CcO·CN); fully reduced CcO (CcO−FR); mixed-valence CcO in complex with CO (MV·CO); [*N*,*N*-bis]2-hydroxyethylglycine (Bicine); *N*-[2-hydroxyethyl] piperazine-*N*′-3-propanesulfonic acid (EPPS); Tris[hydroxymethyl] aminomethane (Tris); 2[*N*-morpholino]-ethanesulfonic acid (Mes); 2[*N*-cyclohexylamino]-ethanesulfonic acid (Ches); 3-[cyclohexylamino]-1 propanesulfonic acid (CAPS); ethylenediaminetetraacetic acid (EDTA); 3-acetylpyridine adenine dinucleotide reduced form (apNADH); phenazine methosulfate (PMS); Triton X 100 (TX-100); *n*-dodecyl-*β*-D-maltoside (DM).

10.1021/bi048435c CCC: $30.25
Published on Web 02/19/2005

We had noticed earlier that in CcO−O the pK_a of the group influencing the spectrum of heme a_3 is close to 7 (*3*). This raises the question, "Does the optical response of heme a_3 to pH changes and the pH-dependent reactions with heme a_3 have the same origin?" Both phenomena might be a reflection of one and the same protolytic group involved in events at the binuclear center. In this case the identification of this group and the mechanism of its interaction with the binuclear center would be of value in elucidating of the catalytic role of this group.

The present study suggests that the surface-exposed Glu60 from subunit II, localized at the entrance of the proton conducting K-channel, is a likely candidate for the residue that interacts with both heme *a* and heme a_3 in oxidized CcO. We also suggest that when this residue is protonated protons can diffuse through the K-channel and when the residue is deprotonated the channel is closed with a substantial loss in proton conductivity.

MATERIALS AND METHODS

Materials. Bicine, EPPS, Tris, Mes, Ches, CAPS, and Bis-tris buffers with L-histidine, HCl, EDTA, apNADH, PMS, and cresol red sodium salt were from Sigma, bromothymol blue was from Aldrich, peroxide-free Triton X 100 was from Roche Diagnostics, and *n*-dodecyl-β-D-maltoside (DM) was from Anatrace. NaCN was from Mallinckrodt.

Enzyme Purification. Bovine CcO was isolated by the modified method of Soulimane and Buse (*10*) with an introduction of one more step − gel filtration chromatography. This change is a consequence of our observation that extended exposure of CcO to the anion exchanger Sepharose Q modifies the enzyme surface sites for anion binding (*11*). Therefore, we shortened the time that CcO was exposed to Sepharose Q; as this led to incomplete purification an additional step was introduced. Briefly, mitochondria are subjected to the protein extraction twice with Triton X 100. EDTA (1 mM) and histidine (1 mM) were added to the original extraction medium (10 mM Tris, pH 7.6, 250 mM sucrose) to minimize binding of transition metals; the EDTA was omitted in the second extraction. The second extract, containing solubilized CcO, is further purified in two chromatographic steps during which the detergent Triton X 100 is changed to DM. The CcO bound to the Sepharose Q fast flow column was washed with 700 mL of 10 mM Tris, pH 7.6, 0.1% DM and then by 500 mL of the same buffer containing 70 mM K_2SO_4. The CcO is eluted from the column with 200 mM K_2SO_4 in 10 mM Tris, pH 7.6, 0.1% DM. The eluted CcO is concentrated and further purified on a Sephacryl S300HR column using 10 mM Hepes, pH 7.8, 50 mM K_2SO_4 and 0.1% DM as buffer. During this chromatography CcO separates into two fractions. The first fraction contains a small amount of CcO contaminated with other protein. The second, major fraction, containing the purified CcO and used in this study, was also analyzed for a subunit composition and showed the presence of all 13 subunits.

Measurement of Spectral Sensitivity of CcO to pH. Three forms of enzyme were used to examine the sensitivity of CcO to pH: fully oxidized CcO as isolated (CcO−O), the complex of oxidized CcO with cyanide (CcO·CN) and the so-called mixed-valence CcO in a complex with carbon monoxide (MV·CO). In MV·CO cytochrome *a* and Cu_A are oxidized and cytochrome a_3 and Cu_B are reduced and stabilized by the bound CO. MV·CO was prepared from CcO−O that had been made anaerobic by repeated evacuation followed by mixing of the enzyme solution in argon several times. The anaerobic CcO−O was then exposed to CO for about 4 min at room temperature; this was sufficient to convert the enzyme to MV·CO in high yield, typically about 90%. The CcO·CN complex was made by incubation of stock CcO−O (200−240 μM CcO in 10 mM Hepes, pH 7.8, 50 mM K_2SO_4, 0.05% DM) with 10 mM NaCN for 15 min at room temperature.

The effect of pH on the optical spectrum of CcO was measured in two ways. The first was based on the rapid acidification of a basic solution of CcO (4.8 μM CcO, 1 mM Hepes, pH 8.0, 100 mM K_2SO_4, 0.05% DM) by addition of a small amount of concentrated MES buffer. For example, addition of 20 μL of 0.9 M MES to 2 mL of CcO changed the pH from pH 8.0 to pH 5.8. For the MV·CO complex a Thunberg type optical cell was used and MES was added from the sidearm. The spectral changes and the kinetics of this change were monitored using a HP 8453 or HP 8452 diode array optical spectrometers.

For the accurate determination of the dependence of the Soret band position on pH, a second approach was employed. Concentrated CcO (200−240 μM) in 10 mM Hepes, pH 7.8, 50 mM K_2SO_4 and 0.1% DM was diluted to 3.6 μM in 100 mM buffers of different pH values. Again for measurements with MV·CO complex the anaerobic Thunberg type optical cell was used and enzyme, first converted to MV·CO form in the sidearm, was mixed with buffer in the cell. The spectra of CcO−O and MV·CO were taken 20 s after mixing CcO with the buffer. The spectrum of CcO·CN was recorded 240 s after mixing. MES buffer was used for pHs between pH 5.2 and 6.6, Bis-tris between pH 6.8 and 7.2, EPPS from pH 7.4 to 8.6, Ches from pH 8.8 to 9.8 and CAPS from pH 10.0 to 11.0. Each buffer also contained 100 mM K_2SO_4 and 0.1% DM.

To assess the extent of the shift of Soret maximum with pH, we monitored the ratio of absorbances at selected wavelength pairs (Figure 5), one on each side of the Soret maximum. The selected wavelengths were at or very close to the maximum and minimum in the difference spectrum of CcO at pH 5.8 minus that at pH 8.0. For CcO−O the wavelengths were 433 and 411 nm, for the MV·CO complex they were 434 and 426 nm, and for CcO·CN were 421 and 437 nm. There are two advantages to this approach: (i) the ratio is insensitive to slight variations in CcO concentration among the samples, and (ii) it is very sensitive even to small changes of the band which increases the accuracy in the determination of the shift.

The kinetics of the spectral changes of CcO induced by acidification is biphasic, and the rapid phase was too fast to follow in the optical spectrometer. To characterize the process in the rapid phase we utilized a stopped-flow instrument. In the stopped-flow pH jump measurement 13 μM CcO−O in 1 mM Hepes, pH 8.0, 100 mM K_2SO_4, 0.05% DM was mixed with an equal volume of 300 mM Mes buffer, pH 5.7, 100 mM K_2SO_4, 0.05% DM.

Magnetic circular dichroism (MCD) was also used to characterize the effect of pH on both CcO−O and oxidized heme a_3 in complex with cyanide (a^{3+}CN). The MCD spectrum of a^{3+}CN complex was obtained as a difference

of the spectra of oxidized CcO·CN complex and CcO−O (*12*). Prior to MCD measurements CcO·CN complex was incubated at pH 5.8 for 4 min to completely develop the spectral change (Figure 1C). MCD spectra were recorded on a Jasco 500C spectropolarimeter equipped with a 1.3 T electromagnet.

Optical difference spectra of reduced *minus* oxidized heme *a* and heme a_3 at pH 8.0 and pH 5.8 were calculated from four recorded spectra: CcO−O ($a^{3+}a^{3+}$), oxidized CcO·CN ($a^{3+}a^{3+}$CN), fully reduced CcO ($a^{2+}a_3{}^{2+}$), and the reduced complex of CcO·CN ($a^{2+}a^{3+}$CN) where heme a_3 is stabilized in oxidized state by cyanide. The spectrum of a^{2+} *minus* a^{3+} was calculated as the difference of $a^{2+}a^{3+}$CN *minus* $a^{3+}a^{3+}$CN and spectrum of $a_3{}^{2+}$ *minus* $a_3{}^{3+}$ as a difference of ($a^{2+}a_3{}^{2+}$ *minus* $a^{3+}a^{3+}$) *minus* (a^{2+} *minus* a^{3+}). The reduction of CcO was achieved in anaerobic conditions by addition of about 1 mg of solid dithionite. 10 mM NaCN was present in all CcO·CN samples. The pH of each sample of reduced oxidase was verified after the spectrum was recorded.

Proton Stoichiometry Measurements. pH changes in the solution were measured during the conversion of CcO−O to MV·CO and CcO−O to fully reduced CcO (CcO−FR). All pH changes associated with the redox transitions of CcO were recorded optically under anaerobic conditions using pH-sensitive dyes. For conversion of CcO−O to CcO−FR typically 2 mL of CcO−O in a weakly buffered solution, containing both the pH indicator and the mediator PMS, was made anaerobic by replacing air by argon as described above. Reduction was initiated by addition of apNADH to CcO−O from the sidearm of the anaerobic optical cell. The conversion of CcO−O to MV·CO was monitored as follows. The solution of CcO−O plus pH-sensitive dye was made anaerobic in the optical cell then briefly evacuated and CO was admitted. The reaction of CcO with CO was initiated by quick mixing the solution in the CO atmosphere. The evolution of pH changes, reduction of CcO, oxidation of apNADH, and formation of MV·CO were recorded simultaneously at selected wavelengths with the HP 8453 diode array spectrometer operated in a multiwavelength kinetic analysis mode.

pH changes associated with full reduction of CcO were measured at pH 8.2, pH 6.8, and pH 5.8. All samples contained 4−5 μM CcO in 200 μM Hepes, 0.5 μM PMS, 100 mM K_2SO_4, and 50 μM of the appropriate pH indicator. At basic pH (pH 8.0−8.2) the indicator was cresol red, while bromothymol blue was used at both pH 5.8 and pH 6.8. In the experiment at pH 8.2 the buffer was 50 μM Bicine. 50 μM MES was the buffer at both pH 6.8 and pH 5.8. For pH measurements during the conversion of CcO−O to MV·CO the same buffer solutions were used at all three pH values except that PMS was omitted and at pH 8.0 the buffer was 200 μM Tris only. To correlate the absorbance changes of the dye to the number of protons involved a known amount of HCl was added to the reaction mixture at the end of the reaction.

For calculation of the stoichiometry of proton uptake by CcO during full reduction, we assumed that the two-electron oxidation of apNADH proceeds with the release of one proton. In the conversion of CcO−O to MV·CO two reactions contribute to pH changes. First, CO interacts with oxidized catalytic center of CcO according to the reaction (*13*):

$$H_2O + CO \rightarrow CO_2 + 2\,H^+ + 2\,e^-$$

Two electrons are trapped in the catalytic center (heme a_3 and Cu_B) by the binding of a second molecule of CO. The CO_2 that is released is hydrated, and in the pH range 5.8−8.0 the carbonic acid that is produced dissociates:

$$CO_2 + H_2O \Leftrightarrow H_2CO_3 \Leftrightarrow H^+ + HCO_3{}^-$$

According to this reaction mechanism one CO_2 is released for each MV·CO complex formed. A pK_a for H_2CO_3 of 6.37 (*14*) was used in calculations to estimate the contribution of the dissociation of carbonic acid to the pH change of the sample at each pH. From the measured values of proton release plus the calculated contribution of CO_2 to the pH change of the solution, we determined the number of protons taken up from the medium during reduction of the catalytic center.

The concentrations of CcO−O, MV·CO, CcO−FR, and apNADH were established from the optical spectra using the following extinction coefficients: $A_{424} = 156\ mM^{-1}\ cm^{-1}$ for oxidized CcO−O, the difference coefficient $\Delta A_{432-412} = 102.5\ mM^{-1}\ cm^{-1}$ for MV·CO *minus* CcO−O, the difference coefficient $\Delta A_{445-420} = 217\ mM^{-1}\ cm^{-1}$ for CcO−FR *minus* CcO−O and the apNADH concentration was obtained from absorbance at 365 nm with $A_{365} = 9.1\ mM^{-1}\ cm^{-1}$ (*15*). All measurements were performed at 23 °C.

RESULTS

Rapid acidification of a solution of CcO−O from pH 8.0 to pH 5.8 by addition of a small amount of concentrated acid causes changes in the optical spectrum (Figure 1A,B). The difference spectrum of CcO−O taken 20 s after acidification to pH 5.8 *minus* the initial spectrum, recorded at pH 8.0, shows a maximum at 410 nm and a minimum at 430 nm in the Soret region (Figure 1A). The equal amplitudes at these wavelengths indicate that there is a blue shift of the Soret band without a noticeable change in intensity. In the visible range, the maxima are located at 542, 588, and 643 nm and the minima at 558, 610, and 669 nm and represent shifts of the 650 nm and the α and β bands of oxidized CcO (Figure 1B).

The kinetics of the spectral change induced by lowering the pH exhibits two phases (Figure 1C). The first rapid phase was completely developed during the manual mixing following addition of acid. At the end of this phase, the Soret maximum, originally at 424 nm, is shifted to 422 nm. The subsequent second phase also corresponds to a blue shift of the Soret band, but it evolves more slowly, with a rate constant ca. $6 \times 10^{-3}\ s^{-1}$.

The spectral response of CcO to pH change is dependent on the state of binuclear center. Two derivatives of CcO, the complex of oxidized oxidase with cyanide (CcO·CN) and MV·CO in which the reduced binuclear center is stabilized by carbon monoxide, demonstrate this dependence (Figure 1). The most striking is the loss of pH sensitivity of the optical spectrum in the MV·CO complex (Figure 1A,B). We ascribe a relatively small change observable in the Soret region (Figure 1A) to the presence of some residual CcO−O in the MV·CO sample. This assignment is based on the position of minimum at 430 nm and maximum and 410 nm

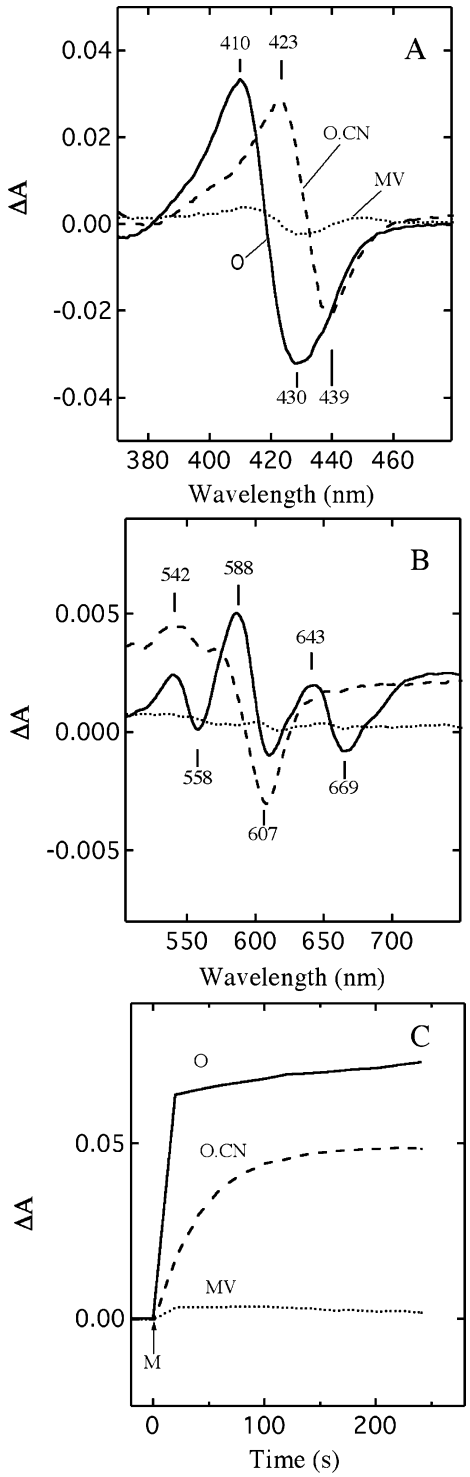

FIGURE 1: Difference spectra and kinetics of spectral response of oxidized CcO, CcO·CN, and MV·CO to a rapid decrease in pH. 4.8 μM oxidase at pH 8.0 (1 mM Hepes, 100 mM K_2SO_4, 0.05% DM) was acidified to pH 5.8 by the addition of 20 μL of 0.9 M Mes. Difference spectra of CcO taken after addition of Mes using as reference the spectrum of the enzyme solution at pH 8.0. Spectra of oxidized CcO (O, solid line) and MV·CO (MV, dotted line) were recorded 20 s after the pH decrease. For the complex of CcO with cyanide (O·CN, dashed line) the spectrum is taken after 240 s and in this case 10 mM NaCN was present in the buffer. (A) Spectra in Soret band. (B) Spectra in visible region; the latter were smoothed. (C) Kinetics of the spectral change in the Soret band from the same experiments. M indicates the addition of Mes. The kinetics were recorded for oxidized CcO as the difference in absorbance at 410 nm *minus* 430 nm ($\Delta A_{410-430}$), for complex with cyanide as $\Delta A_{422-440}$ and for MV·CO complex as $\Delta A_{422-436}$.

in the difference spectrum (Figure 1A) that are the same as those observed with CcO−O. The amplitude corresponds to about 10% of residual CcO−O.

The difference spectrum of CcO·CN (acidic *minus* basic) exhibits a blue shift in the Soret band with a maximum at 423 nm and minimum at 439 (Figure 1A). At 607 nm an absorption decrease is observed (Figure 1B). This spectrum was recorded 240 s after the pH was lowered and the spectral response was completely developed. However, the amplitude in the Soret region is only about two-thirds of that seen with CcO−O (Figure 1), and the spectral response of CcO·CN develops at a substantially slower rate than that of CcO−O (Figure 1C). The kinetics of this change can be fitted with one exponential using a rate constant of $(2.7 \pm 0.3) \times 10^{-2}$ s^{-1}. It was also verified that the presence of 10 mM cyanide does not have an effect on the kinetics or the amplitude of the absorption change. For this demonstration, the free cyanide was removed by gel filtration of the CcO·CN sample. The sample lacking free cyanide exhibited the same characteristics as the sample with cyanide present in solution.

That the spectral change of CcO·CN does not reflect the oxidation of some small population of heme a^{2+} induced by the pH decrease is based on three observations. First, the extrema in the difference spectrum of CcO·CN are at 423 and 439 nm, while the change in the redox state of heme *a* is associated with the extrema at 444 nm and 426−428 nm (see, for example, Figure 4A). Second, were the spectral change of CcO·CN caused by oxidation of heme a^{2+}, we estimate that about 8% of heme *a* (0.4 μM) should be in the reduced state in the CcO·CN complex at pH 8.0. This quantity would be readily detectable in the MCD spectrum of CcO·CN with its characteristic maximum at 452 nm (*12*); this we did not observe. Third, the spectral pH response of CcO·CN is not affected by the presence of 0.5 mM ferricyanide plus 0.1 μM cytochrome *c* in the sample solution which would rapidly oxidize any reduced enzyme present.

To characterize the kinetics of the rapid phase, we subjected CcO−O to a pH jump in the stopped flow apparatus. The blue shift of the Soret band following a pH change from 8 to 5.7 was measured at 410 nm (Figure 2A). The rapid phase is a two-exponential process, and the rate constants obtained from fitting are 7 ± 1 and 0.8 ± 0.1 s^{-1} with relative contributions of 84 and 16%, respectively.

The spectral response of CcO−O induced by acidification can be reversed (Figure 2B). The pH of a sample of CcO−O was rapidly lowered from 7.8 to 5.6 and then returned back to 7.8. The difference spectrum in the Soret region between the initial CcO at pH 7.8 and CcO after pH cycling has extrema at 401 and 438 nm. However, the residual amplitude is no more than 6% of that observed during pH lowering indicating that irreversible spectral changes on this time scale are small.

The absence of any pH sensitivity in the MV·CO derivative would appear to implicate heme a_3 as the only pH-sensitive component. However, the Soret band has contributions from both heme *a* and heme a_3, and these two hemes are not resolved in the optical spectrum of CcO−O. To establish which of the hemes is pH-sensitive, we employed both MCD and the optical difference spectroscopy.

The MCD spectrum of CcO−O in the Soret region is due to low-spin heme *a* (*12*); heme a_3 only contributes to the MCD when it is converted from the high-spin to the low-

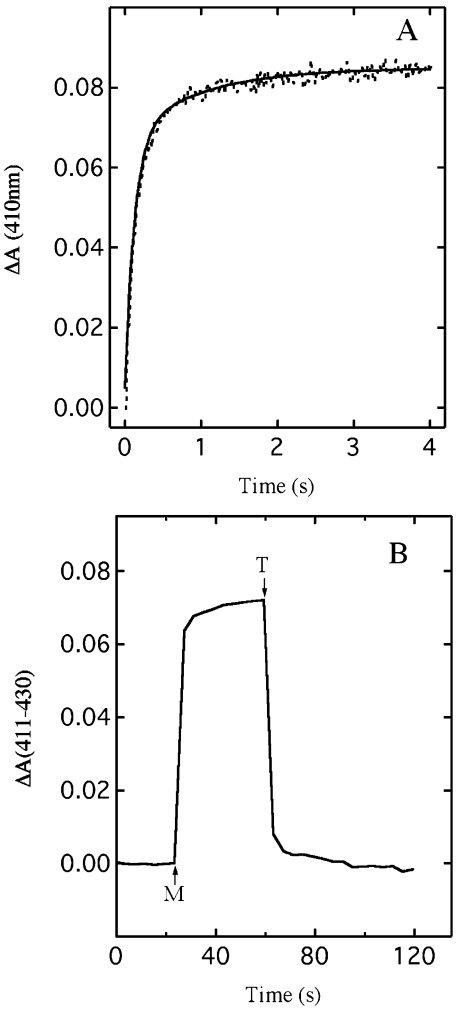

FIGURE 2: Kinetics of spectral change of oxidized CcO produced by a pH jump and reversibility of spectral changes. (A) Kinetics of the spectral changes of oxidized CcO measured at 410 nm following a pH jump in the stopped-flow. 13 μM oxidized CcO at pH 8.0 (1 mM Hepes, 100 mM K_2SO_4, 0.05% DM) was mixed with buffer at pH 5.7 (300 mM Mes, 100 mM K_2SO_4, 0.05% DM). Dashed line; data. Solid line; two exponential fit. (B) Kinetics of spectral response of oxidized CcO induced by a reversible pH change. pH of solution of oxidized CcO (4.8 μM) was rapidly decreased from pH 7.8 to pH 5.6 by adding 20 μL of 0.9 M Mes (M) and then returned back to pH 7.8 by adding 20 μL of 2 M Tris (T).

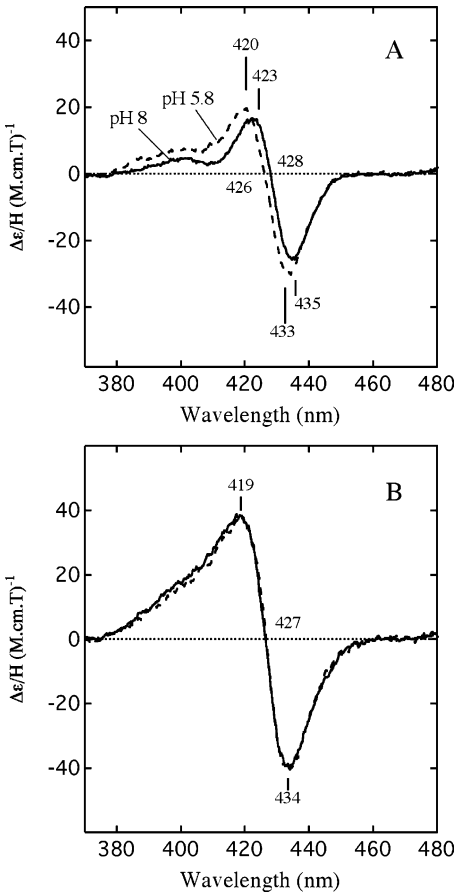

FIGURE 3: Magnetic circular dichroism (MCD) spectra of oxidized CcO and oxidized heme a_3 in complex with cyanide at basic and acidic pH. (A) Soret band spectra of oxidized CcO at pH 8.0 and at pH 5.8 (B) Spectra of heme a_3 in complex with cyanide at pH 8.0 (solid line) and at pH 5.8 (dashed line). 10 mM NaCN was present in both samples. Buffer at pH 8.0: 50 mM Hepes, 100 mM K_2SO_4, 0.05% DM and 50 mM Mes, 100 mM K_2SO_4, 0.05% DM at pH 5.8. Concentration of oxidase − 4.8 μM. For more details see Materials and Methods.

spin state by addition of cyanide (*12*). The MCD spectrum of CcO−O has a derivative shape (Figure 3A) and the MCD zero-crossing corresponds closely to the maximum in the absorption spectrum of the contributing species. At pH 8.0 the positive and negative extrema are at 423 and 435 nm, respectively, with a zero-crossing at 428 nm (Figure 3A). At pH 5.8 the extrema are at 420 and 433 nm and the zero-crossing is at 426 nm (Figure 3A). When pH of the sample is changed from 5.8 to 8.0 the zero-crossing is moved from 426 to 428 nm. This observation indicates that the absorption maximum of heme *a* experiences a reversible shift of 2 nm between pH 8.0 and 5.8.

The behavior of oxidized heme a_3 complexed with cyanide (a_3^{3+}CN) is opposite to that of heme *a* (Figure 3B). The MCD spectrum at pH 8.0 is essentially the same as that at pH 5.8. At both pH values the zero-crossing is at 427 nm and shows that the parent optical spectrum of a_3^{3+}CN is pH-insensitive in the range tested. The positive and negative extrema are at 419 and 434 nm, respectively.

That the optical spectrum of heme *a* and unligated heme a_3 is dependent on pH is documented in Figure 4. At pH 8.0 the difference spectrum of reduced *minus* oxidized heme *a* ($a^{2+} - a^{3+}$) (Figure 4A) has a minimum at 428 nm. At pH 5.8 the minimum is at 426 nm. At both pH values the maximum is at 446 nm. Very similar behavior is observed for heme a_3 (Figure 4B). At pH 8.0 the minimum in the difference spectrum ($a_3^{2+} - a_3^{3+}$) is at 414 nm and at pH 5.8 it is shifted to 412 nm. At both pH values the maximum is at 444 nm.

The minima at 428 and 426 nm observed in the difference spectra of heme *a* ($a^{2+} - a^{3+}$) at pH 8.0 and 5.8, respectively, are the same as the zero-crossing points in MCD spectrum of oxidized heme *a* (Figure 3A). We assume, therefore, that the optical difference spectra also indicate the true position of maxima in the absolute spectra of oxidized heme *a*. From this we conclude that the maximum of oxidized heme a_3, located at 414 nm at pH 8.0, is shifted to 412 nm at pH 5.8. Thus both hemes experience the same 2 nm shift when the pH is changed from 8.0 to 5.8.

The pH dependence of the position of the Soret band, represented by the absorbance ratio, in the pH range between

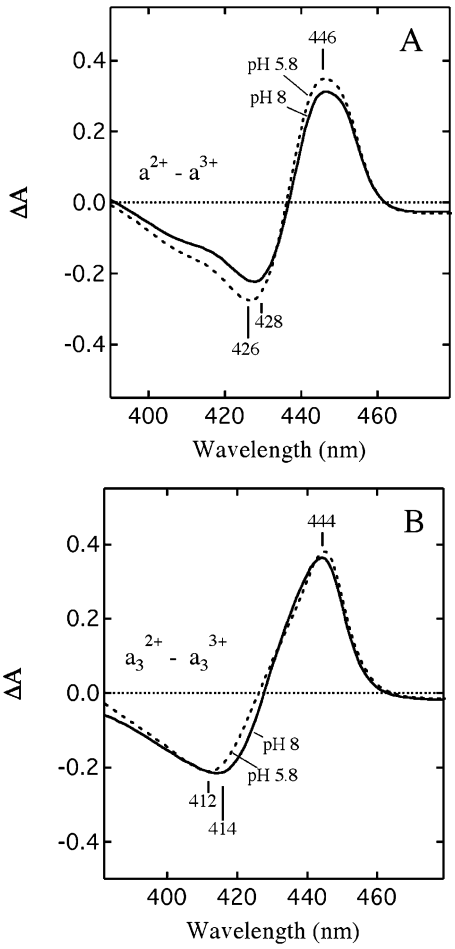

FIGURE 4: Optical difference spectra of reduced *minus* oxidized for both heme *a* and heme a_3 at pH 8.0 and pH 5.8. (A) The difference spectra of heme a^{2+} *minus* heme a^{3+}. (B) The difference spectra of heme a_3^{2+} *minus* heme a_3^{3+}. Solid lines: spectra at pH 8.0. Dashed lines: spectra at pH 5.8. Conditions are the same as in Figure 3. For more details see Materials and Methods.

5.5 and 9.0 reveals one transition for both CcO−O and CcO·CN (Figure 5). The spectral dependencies, determined for three different preparations of CcO, could be fitted to a sigmoidal function consistent with the ionization of a single group with a pK_a = 6.6 ± 0.2 for CcO−O and a pK_a = 6.8 ± 0.1 for CcO·CN. However, for the MV·CO complex in the pH range between pH 5.5 and 11.0 there was no well-defined transition of the Soret band. The spectrum exhibited only a slight monotonic dependence on pH.

To examine if the lack of pH sensitivity of MV·CO is due to a shift in pK_a of the protolytic group following reduction of heme a_3 plus Cu_B we measured proton uptake during conversion of CcO−O to both MV·CO and to CcO−FR. These measurements were made at three different pH values, 5.8, 6.8, and 8.0 in the case of MV·CO and 5.8, 6.8, and 8.2 in the case of CcO−FR. Representative kinetics for the conversion of CcO−O to MV·CO and of CcO−O to CcO−FR together with the associated pH changes at basic pH are displayed in Figure 6.

The transition of CcO−O to MV·CO was observed as a relative spectral change ΔA(432−414 nm) (Figure 6A). In the same sample pH measurement, recorded as the absorbance difference, ΔA(528−700 nm), reveals that there is a simultaneous acidification of the solution (Figure 6A). The control sample, prepared without a pH indicator, showed that

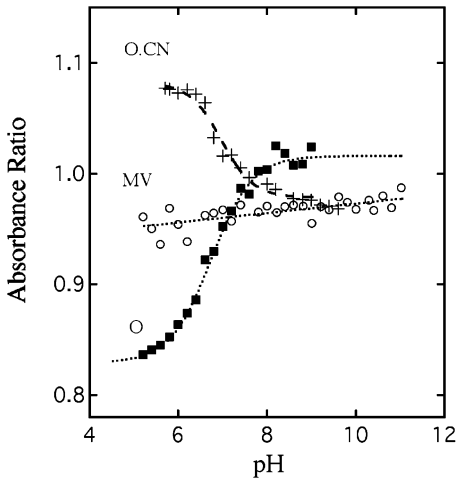

FIGURE 5: pH dependence of the position of Soret band, represented by the absorbance ratio, for oxidized CcO, CcO·CN, and MV·CO. 240 μM CcO in 10 mM Hepes, pH 7.8, 50 mM K_2SO_4 and 0.1% DM was diluted to 3.6 μM in 100 mM buffers at different pH values and optical spectra were taken 20 s after mixing CcO with the relevant buffer for oxidized CcO (O) and MV·CO (MV). For CcO·CN (O·CN) the spectra were collected 240 s after dilution. Each point is a fresh sample. Symbols are data and the lines are fits to the data. For CcO−O and CcO·CN the best fit is to a single group with pK_a values of 6.6 and 6.8, respectively. A linear fit is used for MV·CO. For more details see Materials and Methods.

there is basically no spectral contribution from oxidase at the wavelengths selected to monitor the pH changes (Figure 6A).

The kinetics of the full reduction of CcO−O at pH 8.2 was monitored as the absorbance difference ΔA(445−420 nm) (Figure 6B) and the changes in pH were monitored using the absorption changes at 562 *minus* 700 nm. After addition of the reductant (apNADH) an instantaneous and variable spectral change was observed in the ΔA(562−700 nm). During this time the reduction of CcO was less than 3% and so we assume that this initial change is a mixing artifact. Only the spectral changes following this initial event were considered to be associated with the reduction reaction. When reduction was complete the enzyme was reoxidized by admitting air to the cuvette. As the reaction is accompanied by proton uptake the amount of protons consumed was quantified by the addition of a known amount of HCl (Figure 6B). Similar kinetic measurements were performed at pH 6.8 and pH 5.8. From these data the number of protons taken up in the transition of CcO−O to MV·CO and also to CcO−FR was established (Figure 7). The results are summarized in Table 1.

DISCUSSION

Prolonged incubation of CcO at acidic pH leads to the form of the enzyme called "slow". This process and the "slow" form of the enzyme have been extensively investigated in the past (*16*−*20*). Those studies showed that in the "slow" enzyme the catalytic binuclear center, composed of heme a_3 and Cu_B, is modified and that this form of enzyme cannot be involved in catalysis. However, the overall spectral change of oxidized CcO following acidification is composed of at least two phases (Figure 1C). The first and rapid spectral change may well have relevance to the function of CcO and is characterized in the present work.

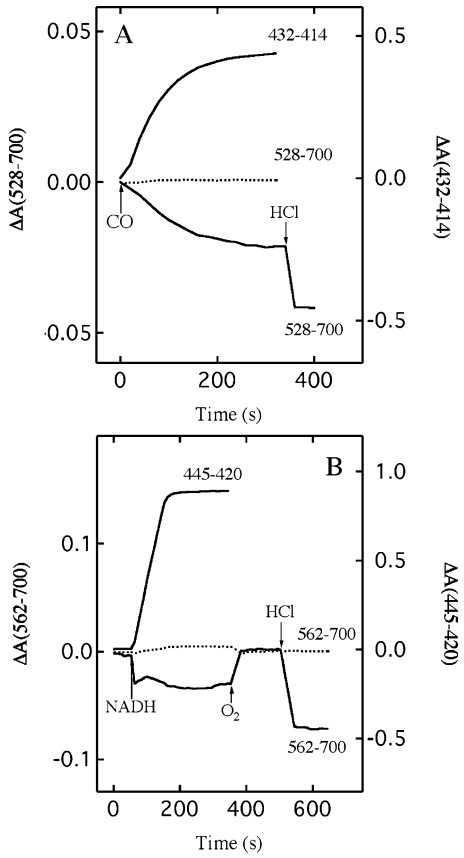

FIGURE 6: pH changes accompanying the conversion of CcO−O to MV·CO and of CcO−O to fully reduced enzyme at basic pH. (A) Conversion of CcO−O to MV·CO. 4.6 μM CcO−O at pH 8.0 (0.1 mM Tris, 100 mM K_2SO_4, 0.1% DM, 40 μM cresol red) was exposed to CO anaerobically. Selected wavelength pairs were used to monitor two parameters: formation of MV·CO relative to CcO−O ($\Delta A_{432-414}$) and pH changes ($\Delta A_{528-700}$). (—) in the presence of CcO; (- - -) in its absence. At the end of the reaction the pH changes were calibrated by addition of a known amount of HCl. (B) Full reduction of CcO−O. 4 μM CcO at pH 8.2 (200 μM Hepes, 50 μM Bicine, 0.5 μM PMS, 100 mM K_2SO_4, 0.1% DM, and 50 μM of cresol red) was reduced anaerobically. The wavelength pair 445 nm *minus* 420 nm monitors the formation of fully reduced CcO relative to CcO−O following addition of 8.5 μM apNADH. The wavelength pair 562 nm *minus* 700 nm monitors the pH changes during the reduction (—). As control the spectral changes in 100 mM Bicine solution were recorded (- - -). At the end of reaction, the sample was exposed to oxygen; after a small delay a known amount of acid was added.

During the rapid spectral change of CcO−O following a pH decrease from pH 8.0 to 5.8 the maximum of the Soret band shifts from 424 to 422 nm. The MCD and difference optical spectra of heme *a* and heme a_3 in this region (Figures 3 and 4) show that both hemes experience a 2 nm blue shift in the location of their respective maximum.

In the MV·CO complex both hemes appear to be unaffected by pH changes (Figures 1 and 5). However, in CcO·CN the MCD spectrum of heme a_3 complexed with cyanide indicates (Figure 3B) that only the sensitivity of heme a_3 to pH is lost. Thus the pH-induced spectral change of CcO·CN is due to heme *a*. The subtraction of this difference spectrum of heme *a* from the difference spectrum of CcO−O gives the contribution of heme a_3 to the overall spectral change. The spectra of both heme *a* and heme a_3 display a blue shift in the Soret band (Figure 8).

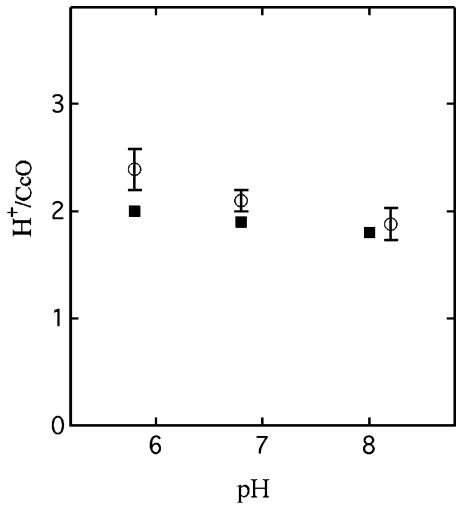

FIGURE 7: pH dependence of the stoichiometry of proton uptake during formation of MV·CO (■) and fully reduced CcO (○) from CcO−O. For clarity the error bars are omitted in the MV·CO data. For experimental details see Materials and Methods.

Table 1: Proton Uptake by Oxidase during the Transition from Oxidized CcO to MV·CO and to the Fully Reduced Form (CcO−FR)[a]

	H^+/CcO		
	pH 5.8	pH 6.8	pH 8.2
MV·CO	2 ± 0.3 (3)	1.9 ± 0.3 (3)	1.8 ± 0.2[b] (2)
CcO−FR	2.4 ± 0.2 (4)	2.1 ± 0.1 (4)	1.9 ± 0.2 (4)

[a] The number of measurements is given in parentheses. [b] pH was 8.0.

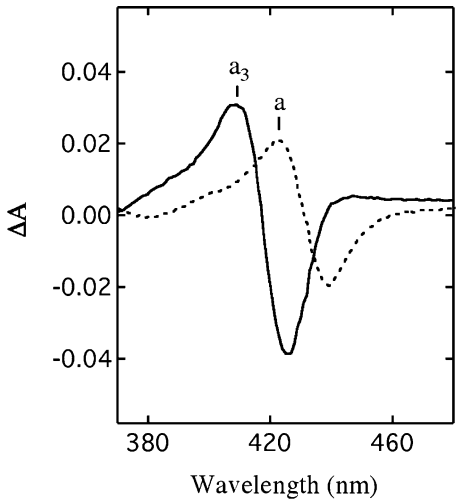

FIGURE 8: Spectral change of oxidized heme *a* and heme a_3 induced by pH decrease. The difference spectra of heme *a* (a) and heme a_3 (a_3) at pH 5.8 versus that at pH 8.0. The heme *a* spectrum is the spectrum of CcO·CN. The spectrum of heme a_3, with extrema at 409 and 426 nm, is the result of subtracting the CcO·CN spectrum from that spectrum of CcO−O. Both spectra are from data presented in Figure 1.

The stopped-flow kinetics of the spectral change following a pH jump from 8.0 to 5.7 is composed of two phases. The contribution of rapid phase ($k = 7$ s^{-1}) to the overall amplitude is about 84% and that of the slow phase ($k = 0.8$ s^{-1}) is 16%. This could be interpreted most simply as the spectral contribution from the two hemes that are developed with different rates. However, we cannot exclude that the

presence of this small slow phase in the kinetics is due to some residual heterogeneity in the population of purified CcO−O.

The dependence of the position of Soret band on pH for both CcO−O and CcO·CN revealed that the observed pH sensitivity can be assigned to the interaction of the hemes with a single protolytic group (Figure 5). In CcO−O the group is characterized by a pK_a of 6.6 ± 0.2 and in CcO·CN the pK_a was found to be 6.8 ± 0.1 (Figure 5). Because the two pK_a values are almost the same we assume that both hemes are influenced by the ionization state of one and the same group. The small increase in pK_a in CcO·CN we ascribed to the cyanide treatment of CcO−O.

The pK_a of 6.6 differs from the value of 7.8 previously identified for oxidized heme a_3 from optical spectra of the bovine enzyme (*4*). However, the conditions in the two sets of experiments are not comparable. The pK_a of 7.8 was established in experiments that recorded the optical spectra of CcO−O after several hours of incubation at different pH values at which time an equilibrium in the spectral evolution had been reached.

The lack of pH sensitivity of the MV·CO complex between pH 5.5 and 11.0 (Figure 5) could be a result of an increase in the pK_a of the interacting group following reduction of the catalytic center. In this case the pK_a should be dependent on the redox state of the catalytic center and when this center is reduced the pK_a is raised from 6.6 to a value greater than 11.0. This implies that there is a strong interaction between the catalytic center and the identified group.

That this does not occur and that the interaction with the group has to be weak is demonstrated by the stoichiometry of proton uptake during the conversion of CcO−O to MV·CO and to CcO−FR (Figure 7, Table 1). At weakly basic pH (8.0−8.2), where the identified group in CcO−O is deprotonated, reduction of the catalytic center should be associated with a proton uptake. However, at pH 5.8 the group is already protonated in oxidized enzyme and reduction should not lead to proton uptake by the same group. Consequently the stoichiometry of proton uptake should decrease with decreasing pH. The observed behavior is opposite and there is no reduction in proton consumption with a decrease in pH (Figure 7, Table 1).

At all pH values tested the formation of the MV·CO complex is associated with the uptake of close to 2 H^+/CcO from the bulk phase. These two protons are assumed to compensate the charge of the two electrons delivered to heme a_3 and Cu_B keeping the catalytic center in the electrically neutral state (*21*). In the course of full reduction of CcO we observed a small increase in proton uptake above 2 H^+/CcO as the pH is decreased. This small increment above 2 is consistent with published data that has shown a small, pH-dependent, and nonstoichiometric proton uptake coupled with reduction of heme *a* and Cu_A (*22*).

From the proton uptake measurements we conclude that the pK_a of the group is independent of the redox state of heme a_3 − Cu_B, or of the redox state of heme *a* or Cu_A. The data also implies that the group has to be located more distant from the redox centers and consequently poses a question about the mechanism of interaction.

There are two possible mechanisms for the interaction of the protolytic group with hemes. The first is a direct electrostatic interaction between the two centers, while the second is an indirect interaction in which charge changes are propagated between these sites by the protein. The second mechanism is the case when the change in the ionization state of a protolytic group triggers a conformational event that leads to the spectral change. Our conclusion, based on the arguments that are presented below, is that direct electrostatic interaction is unlikely.

First, a group that is in a rapid acid−base equilibration with the solvent, for example, located on the enzyme's surface, and involved in direct electrostatic interaction with hemes can be excluded. This conclusion is based on the slow rate of the spectral relaxation following the pH jump (Figure 2A). For such a group the protonation (*23*) and the associated spectral change would have been developed within the dead time of stopped-flow instrument.

The only scenario in which an electrostatic interaction is operational is that the relevant residue is slowly accessible to protons. For example the sensitive group is buried within the protein and the slow spectral relaxation reflects slow proton diffusion to this group. This possibility, however, is contradicted by the behavior of CcO·CN. In this derivative the ionizing group is accessible to protons from the bulk aqueous phase because the spectrum of heme *a* responds to pH changes (Figures 1 and 4A) while heme a_3 does not. With an electrostatic interaction in place both hemes should be sensitive to pH. These arguments lead to the conclusion that the interaction between the group and the hemes has to be mediated by protein.

To get more specific insight into the mechanism of interaction the identity of this group and its location will be helpful. Our preliminary kinetic studies of CcO reduction offer additional information for identifying the group. When oxidized CcO is reduced anaerobically with excess reductant (dithionite plus hexamine ruthenium) the limiting rate of reduction of heme a_3 is pH dependent, being maximal at acid pH and decreasing rapidly with increasing pH. The data are consistent with a group with a pK_a of 6.5 regulating the intramolecular electron transfer to heme a_3. (M. Antalik, M. Fabian, and G. Palmer, preliminary results). Altogether the data on the rate of heme a_3 reduction and the spectral sensitivity of hemes indicate the involvement of a single protolytic group with essentially the same pK_a.

The current picture is that the rate of electron transfer to heme a_3 in anaerobic conditions is limited by proton delivery to the catalytic site (*24*). There are two proton conducting channels that connect the matrix phase of mitochondria with the binuclear center, called the D and the K channels (*2*; reviews refs *25*−*27*). The K-pathway appears to be used for proton uptake during the reduction of the catalytic center and prior to its interaction with oxygen (*28*−*33*). This fact restricts the possible location of the protolytic group to the K-pathway. Taking into consideration the identified pK_a of 6.6 the most obvious candidate for the pertinent residue would be His256 of subunit I. This residue is located close to the entry of proposed K-channel in bovine CcO (*2*). However, mutation of the corresponding histidine in bacterial oxidases showed that this residue is not required for proton delivery to the binuclear center (*34*, *35*). Surprisingly, it was found that the surface-exposed glutamic acid present in subunit II in *Rhodobacter sphaeroides* oxidase (Glu101, Glu60 in bovine enzyme) facilitates proton diffusion through the K-channel (*35*). Given these observations, we suggest

that Glu60 as the group in the K-channel responsible for the pH sensitivity of both hemes. This suggestion requires that the pK_a of Glu60 be a little more than two pH units higher than is the pK_a of free Glu. As the glutamate in question is surrounded by a large number of nonpolar residues such an increase in pK_a is not unreasonable.

With Glu60 as the presumed protolytic residue we propose that the interaction between the residue and both hemes is propagated through a hydrogen bonded network. To explain the lack of pH sensitivity of MV·CO complex we assume that the hydrogen bond network is disrupted at some point between Glu60 and the hemes. This disruption of the hydrogen bond network might occur at Lys319 that has been proposed to undergo movement to compensate for the charge of electrons delivered to the catalytic center (*36*). Similarly, binding of cyanide to heme a_3 in oxidized CcO results in the selective disruption of network between the Glu60 and heme a_3 and at the same time slows down the response of heme *a* to pH change.

What is the possible relevance of Glu60 to the catalytic reaction? As mentioned above the group regulates proton access to the binuclear center. With our preliminary data on the reduction of heme a_3 we can add that when this group is protonated the K-pathway is open and proton access is rapid. Conversely, when the group is deprotonated the access of protons to the catalytic site is blocked. This idea can also be used to explain the pH-dependent yield of the two catalytic intermediates, P and F. In the reaction of CcO−O with hydrogen peroxide the relative yields of P and F are controlled by a group with a pK_a of 6.6−6.8 (*8*, *9*). This dependence is observed only in the interaction of CcO−O with a low concentration of H_2O_2 (μM) in small molar excess; the reaction sequence is probably:

$$\text{CcO}-\text{O} + \text{H}_2\text{O}_2 \Rightarrow \text{P} \Rightarrow \text{F} \Rightarrow \text{CcO}-\text{O}$$

The yields of P and F are determined at the moment when all the CcO−O has reacted with H_2O_2 and at all pH values studied the product is a mixture of P and F (P/F). With constant concentrations of CcO−O and H_2O_2 the rate of reaction is, at most, only very weakly dependent on pH. However, the relative yields of P and F are pH dependent. F dominates at acidic pH and with increasing pH the amount of F decreases with a concomitant increase of P. We explain this dependence by assuming that the rate of P formation is pH independent and that the rates of the P ⇒ F and F ⇒ CcO−O conversions determine the relative yield of the P and F forms.

We previously showed that the pH-dependent rate of the P ⇒ F transition is not influenced by a group with a pK_a around 6.6 (*37*) and the apparent rate constant for the P ⇒ F transition increases linearly with the increasing proton concentration (*37*). In contrast the rate of decay of F ⇒ CcO−O is under control of a single group with a pK_a of 6.8 and the pH dependence is very similar to that described above for heme a_3 reduction (M. Fabian and G. Palmer, preliminary data). Thus it appears that the F ⇒ CcO−O conversion requires proton uptake through the K-channel and that a group with a pK_a close to the observed value of 6.6 controls the rate of proton diffusion to the catalytic center. These data indicate that at acidic pH, where the group with a pK_a of 6.6 is protonated, the P ⇒ F transition is more rapid than F ⇒ CcO−O and there is consequently an accumulation of the F form. At basic pH, both the conversion of P ⇒ F and F ⇒ CcO−O are slowed. However, the decay of F ⇒ CcO−O is relatively faster than the conversion of P ⇒ F and this causes accumulation of P relative to F at basic pH.

The final comment concerns the stoichiometry of proton uptake and its pH dependence. The previously determined stoichiometry of proton uptake, accompanying full reduction of CcO, varies between 1.8 H^+ and 2.8 H^+/CcO at basic pH (*21*, *38*−*41*). This stoichiometry decreases with decreasing the pH and at pH 6.2 it is about 1 H^+/CcO (*41*). However, we have one observation, based on the reaction of MV·CO with oxygen, that this stoichiometry should not decline at acidic pH. We prepared the MV·CO complex at both pH 8.0 and pH 5.8 and after mixing the samples with air the reaction with O_2 was initiated by photolysis. The product of the reaction is the relatively stable P form. This formation of P involves only internal proton transfer without proton uptake from the bulk solution (*42*). Thus if the number of protons at the binuclear center of MV·CO were different at pH 5.8 than that at pH 8.0 different reaction products would have been expected. However, at both pH values we observed the same P form, as judged optically.

ACKNOWLEDGMENT

We would like to thank Dr. A. Musatov for analyzing the subunit composition of cytochrome *c* oxidase.

REFERENCES

1. Kadenbach, B., Jarausch, J., Hartmann, R. and Merle, P. (1983) Separation of mammalian cytochrome-c oxidase into 13 polypeptides by sodium dodecyl sulfate gel electrophoretic procedure, *Anal. Biochem. 129*, 517−521.
2. Tsukihara, T., Aoyama, H., Yamashita, E., Tomizaki, T., Yamaguchi, H., Shinzawa-Itoh, K., Nakashima, R., Yaono, R., and Yoshikawa, S. (1996) The whole structure of 13-subunit oxidized cytochrome *c* oxidase at 2.8 Å, *Science 272*, 1136−1144.
3. Fabian, M., and Malmström, Bo. G. (1989) The effect of pH changes on the optical spectrum of oxidised cytochrome oxidase, *Biochim. Biophys. Acta 973*, 414−419.
4. Papadopoulos, P. G., Walter, S. A., Li, J., and Baker, G. M. (1991) Proton interactions in the resting form of cytochrome oxidase, *Biochemistry 30*, 840−850.
5. Wilson, D. F., Erecinska, M., and Brocklehurst, E. S. (1972) The chemical properties of cytochrome *c* oxiadse in intact mitochondria, *Arch. Biochem. Biophys. 151*, 180−187.
6. Andreev, I. M., and Konstantinov, A. A. (1983) Reaction of oxidized cytochrome *c* oxidase with cyanide. Effects of pH, cytochrome *c*, and the membrane environment, *Bioorg. Chem.* (USSR) (Eng. Trans.) *9*, 101−111.
7. Konstantinov, A., Vygodina, T., and Andreev, I. M. (1986) Electrogenic proton exchange between cytochrome a_3 active center and M-aqueous phase, *FEBS Lett. 202*, 229−234.
8. Vygodina, T., and Konstantinov, A. (1989) Effect of pH on the spectrum of cytochrome *c* oxidase hydrogen peroxide complex, *Biochim. Biophys. Acta 973*, 390−398.
9. Fabian, M., Skultety, L., Jancura, D., and Palmer, G. (2004) Implications of ligand binding studies for the catalytic mechanism of cytochrome *c* oxidase, *Biochim. Biophys. Acta 1655*, 298−305.
10. Soulimane, T., and Buse, G. (1995) Integral cytochrome-c oxidase. Preparation and progress towards a three-dimensional crystallization *Eur. J. Biochem. 227*, 588−595.
11. Fabian, M., Jancura, D., and Palmer, G. (2004) Two sites of interaction of anions with cytochrome *a* in oxidized bovine cytochrome *c* oxidase, *J. Biol. Chem. 279*, 16170−16177.
12. Babcock, G. T., Vickery, L. E., and Palmer, G. (1976) Electronic state of heme in cytochrome oxidase. I. Magnetic circular dichroism of the isolated enzyme and its derivatives, *J. Biol. Chem. 251*, 7907−7919.

13. Bickar, D., Bonaventura, C., and Bonaventura, J. (1984) Carbon monoxide-driven reduction of ferric heme a and heme proteins, *J. Biol. Chem. 259*, 10777−101783.
14. Lange, N. A., Forker, G. M., Burington, R. S. (1946) *Handbook of Chemistry*, p 1377, Handbook Publishers, Sandusky.
15. Kaplan, N. D. (1960) The pyridine coenzymes, in *The Enzymes* (Boyer, P. D., Lardy, M., and Myrbäck, K., Eds.) p 105, Academic Press, New York.
16. Baker, G. M., Noguchi, M., and Palmer, G. (1987) The reaction of cytochrome oxidase with cyanide. Preparation of the rapidly reacting form and its conversion to the slowly reacting form, *J. Biol. Chem. 262*, 595−604.
17. Palmer, G., Baker, G. M., and Noguchi, M. (1988) The rapid and slow forms of cytochrome oxidase, *Chem. Scr. 28A*, 41−46.
18. Schoonever, J. R., and Palmer, G. (1991) Reaction of formate with the fast form of cytochrome oxidase: A model for the fast to slow conversion, *Biochemistry 30*, 7541−7550.
19. Moody, A. J., Cooper, Ch. E., and Rich, P. R. (1991) Characterization of 'fast' and 'slow' forms of bovine heart cytochrome-c oxidase, *Biochim. Biophys. Acta 1059*, 189−207.
20. Cooper, Ch. E., Junemann, S., Ioannidis, N., and Wrigglesworth, J. M. (1993) Slow ('resting') forms of mitochondrial cytochrome *c* oxiadse consist of two kinetically distinct conformations of the binuclear CuB/*a*3 centre-relevance to the mechanism of proton translocation, *Biochim. Biophys. Acta 1144*, 149−160.
21. Mitchell, R., and Rich, P. R. (1994) Proton uptake by cytochrome *c* oxidase on reduction and on ligand binding, *Biochim. Biophys. Acta 1186*, 19−26.
22. Verkhovsky, M. I., Belevich, N., Morgan, J. E., and Wikström, M. (1999) Proton linkage of cytochrome a oxidoreduction in carbon monoxide-treated cytochrome *c* oxidase, *Biochim. Biophys. Acta 1412*, 184−189.
23. Marantz, Y., Einarsdóttir, O., Nachliel, E., and Gutman, M. (2001) Proton-collecting properties of bovine heart cytochrome *c* oxidase: Kinetic and electrostatic analysis, *Biochemistry 40*, 15086−15097.
24. Verkhovksy, M. I., Morgan, J. E., and Wikström, M. (1995) Control of electron delivery to the oxygen reduction site of cytochrome *c* oxidase: A role for protons, *Biochemistry 34*, 7483−7491.
25. Ferguson-Miller, S., and Babcock, G. T. (1996) Heme/Copper Terminal Oxidases, *Chem. Rev. 96*, 2889−2907.
26. Michel, H., Behr, J., Harrenga, A., and Kannt, A. (1998) Cytochrome *c* Oxidase: Structure and Spectroscopy, *Annu. Rev. Biophys. Biomol. Struct. 27*, 329−356.
27. Gennis, R. B. (1998) Multiple proton-conducting pathways in cytochrome *c* oxidase and a proposed role for the active-site tyrosine, *Biochim. Biophys. Acta 1365*, 8020−2025.
28. Vygodina, T. V., Pecoraro, C., Mitchell, D., Gennis, R., and Konstantinov, A. A. (1998) Mechanism of inhibition of electron transfer by amino acid replacement K362M in a proton channel of *Rhodobacter sphaeroides* cytochrome *c* oxidase, *Biochemistry 37*, 3053−3061.
29. Ädelroth, P., Gennis, R., and Brzezinski, P. (1998) Role of the pathway through K(I-362) in proton transfer in cytochrome *c* oxidase from *R. sphaeroides*, *Biochemistry 37*, 2740−2476.
30. Zaslavsky, D., and Gennis, R. B. (1998) Substitution of lysine-362 in a putative protonconducting channel in the cytochrome *c* oxidase from *Rhodobacter sphaeroides* blocks turnover with O_2 but not with H_2O_2, *Biochemistry 37*, 3062−3067.
31. Wikström, M., Jasaitis, A., Backgren, C., Puustinen, A., and Verkhovsky, M. I. (2000) The role of the D- and K-pathways of proton transfer in the function of haem-copper oxidases, *Biochim. Biophys. Acta 1459*, 514−520.
32. Pecoraro, C., Gennis, R., Vygodina, T. V., and Konstantinov, A. A. (2001) Role of the Kchannel in the pH-dependence of the reaction of cytochrome *c* oxidase with hydrogen peroxide, *Biochemistry 40*, 9695−9708.
33. Bränden, M., Tomson, F., Gennis, R. B., and Brzezinski, P. (2002) The entry point of the K proton-transfer pathway in cytochrome *c* oxidase, *Biochemistry 41*, 10794−10798.
34. Pfitzner, U., Odenwald, A., Ostermann, T., Weingard, L., Ludwig, B., and Richter, O.-M. H. (1998) Cytochrome *c* oxidase (heme aa_3) from *Paracoccus denitrificans*: Analysis of mutations in putative proton channels of subunit I, *J. Bioenerg. Biomemb. 30*, 89−93.
35. Tomson, F., Morgan, J. E., Gu, G., Barquera, B., Vygodina, T. V., and Gennis, R. B. (2003) Substitutions for glutamate 101 in subunit II of cytohrome c oxidase from *Rhodobacter sphaeroides* result in blocking the proton-conducting K-channel, *Biochemistry 42*, 1711−1717.
36. Bränden, M., Sigurdson, H., Namslauer, A., Gennis, R. B., Ädelroth, P., and Brzezinski, P. (2001) On the role of the K-proton-transfer pathway in cytochrome *c* oxidase, *Proc. Natl. Acad. Sci. U.S.A. 98*, 5013−5018.
37. Fabian, M., and Palmer, G. (2001) Proton involvement in the transition from the "peroxy" to the ferryl intermediate of cytochrome *c* oxidase, *Biochemistry 40*, 1867−1874.
38. Hallen, S., and Nilsson, T. (1992) Proton transfer during the reaction between fully reduced cytochrome *c* oxidase and dioxygen: pH and deuterium isotope effects, *Biochemistry 31*, 11853−11859.
39. Ädelroth, P., Ek, M., and Brzezinski, P. (1998) Factors determining electron-transfer rates in cytochrome *c* oxidase: investigation of the oxygen reaction in th *R. sphaeroides* enzyme, *Biochim. Biophys. Acta 1367*, 107−117.
40. Tarasev, M., and Hill, B. C. (2002) Detergent modulation of electron and proton-transfer reactions in bovine cytochrome *c* oxidase, *Arch. Biochem. Biophys. 400*, 162−170.
41. Capitanio, N., Capitanio, G., De Nito, E., Boffoli, D., and Papa, S. (2003) Proton transfer reactions associated with the reaction of the fully reduced, purified cytochrome *c* oxidase with molecular oxygen and ferricyanide, *Biochemistry 42*, 4607−4612.
42. Karpefors, M., Ädelroth, P., Namslauer, A., Zhen, Y. J., and Brzezinski, P. (2000) Formation of the "Peroxy" intermediate in cytochrome *c* oxidase is associated with internal proton/hydrogen transfer, *Biochemistry 39*, 14664−14669.

BI048435C